Supplementary Material

Real-time measurements of product compounds formed through the reaction of ozone with breath exhaled VOCs

Xin Xu[1,2,3], Hongwei Pang[4,5,6], Chao Liu[1,2,3], Kangyi Wang[1,2,3], Gwendal Loisel[4,5,6], Lei Li[1,2,3], Sasho Gligorovski[4,5,6]*, Xue Li[1,2,3]*

[1]Institute of Mass Spectrometry and Atmospheric Environment, Jinan University, Guangzhou 510632, China

[2]Guangdong Provincial Engineering Research Center for On-line Source Apportionment System of Air Pollution, Guangzhou, 510632, China

[3]Guangdong-Hongkong-Macau Joint Laboratory of Collaborative Innovation for Environmental Quality, Guangzhou, 510632, China

[4]State Key Laboratory of Organic Geochemistry and Guangdong Provincial Key Laboratory of Environmental Protection and Resources Utilization, Guangzhou Institute of Geochemistry, Chinese Academy of Sciences, Guangzhou 510640, China

[5]Guangdong-Hong Kong-Macao Joint Laboratory for Environmental Pollution and Control, Guangzhou Institute of Geochemistry, Chinese Academy of Science, Guangzhou 510640, China

[6]Chinese Academy of Science, Center for Excellence in Deep Earth Science, Guangzhou, 510640, China

* corresponding authors

Email: tamylee@jnu.edu.cn; gligorovski@gig.ac.cn

Submitted to Environmental Science: Processes & Impacts

Number of texts	**3**
Number of figures	**7**
Number of tables	**6**

Table of contents

Text S1: Blank sample

For both real and simulated breath samples, the blank sample was prepared by filling zero air into a homemade 40-L Nalophan (Scentroid, Canada) bag (Figure S1). Before being delivered into the reaction chamber, the humidity of zero air was adjusted to the level as same as that in the breath (i.e., relative humidity (RH) 92%–94%) by using a humidifier (Figure S1). Then the zero air was pumped into the reaction chamber at a flow rate of 1.5 L min^{-1} controlled by a sampling pump (FCG-5, YanCheng Galaxy Science & Technology LTD, China).

Text S2: Data analysis

MS Raw data were pretreated as reported before and ions with signal intensity $\geq 2.5 \times 10^5$ a.u. were extracted for further analysis [1]. For cluster analysis, those clusters were defined based on the degree of similarity. In the study, hierarchical analysis in MATLAB (R2018b) was performed to discover *m/z* values sharing the same intensity temporal profiles. The pdist function is used to calculate the distance between every pair of objects (i.e., *m/z* values in our case) in a data set. For a data set made up of m objects, there are $m*(m - 1)/2$ pairs in the data set. The result of this computation is commonly known as a distance or dissimilarity matrix. Once the proximity between objects in the data set has been computed, it can determine how objects in the data set should be grouped into clusters, using the linkage function. The linkage function takes the distance information generated by pdist and links pairs of objects that are close together into binary clusters (clusters made up of two objects). The linkage function then links these newly formed clusters to each other and to other objects to create bigger clusters until all the objects in the original data set are linked together in a hierarchical tree. For data mining, *t*-test (GraphPad Prism 7) was performed

to identify the possible products from O_3 reaction with exhaled human breath containing VOCs. When the p value is < 0.0001, it is considered that there is a significant difference between the two groups of samples [2]. Therefore, $p < 0.0001$ was adopted in this study to determine the potential products resulting from O_3 reaction with breath VOCs. Finally, the element compositions of individual products were given using commercial software Xcalibur (Thermo Scientific, USA).

To identify and characterize the detected aromatic compounds we used the aromaticity equivalent (X_C) which is mathematical parameter calculated as follows [3–5]. Therefore, X_C of the organic compounds, which contain C, H, O, and N in their chemical structures, was calculated as follows:

$$X_C = \frac{2C + N - H - 2mO - 2nS}{DBE - mO - nS} \qquad \text{(Eq-S1)}$$

where m and n represent the fraction of oxygen and sulfur atoms, involved in the π-bonds of a molecular structure [3]. In this study, m and n were set to 0.5, since the ESI- mode is most sensitive to compounds that contain carboxylic functional groups [4]. Threshold values of X_C were set as, $2.50 \leq X_C < 2.71$, and $X_C \geq 2.71$, as criteria for the presence of aromatics or multi-core aromatic compounds in the identified ions, respectively [5–7].

Text S3: Calculation of normalized intensity of products.

In many recent studies, peak abundance comparisons in mass spectrometry have been used to show the relative importance of different types of compounds [5,8–10]. However, the ionization efficiencies of different classes of compounds can vary widely [11], so comparing peak abundances between different compounds is likely to produce uncertainty. Calculation of normalized intensity of product compounds formed during the gas-phase reaction of O_3 with VOCs from exhaled breath was performed by using 2-butanone as a reference compound [12]:

$$C_i = \frac{Int_i}{Int_{BUT}} \times C_{BUT} \quad \text{(Eq-S2)}$$

where C_i is the mixing ratio (pptv or ppbv) of compound i detected during the experiments, Int_{BUT} is the intensity of 2-butanone, Int_i is the intensity of product i, and C_{BUT} is the mixing ratio of 2-butanone, i.e., 2 ppbv.

The calculation of the normalized intensity indicated the occurrence of 17 positive ions and 15 negative ions at mixing ratio higher than 5 pptv, which were assigned to 24 compounds (Table S6). We emphasize the discussion on seven compounds with mixing ratio higher than 100 pptv which were observed in both cases i.e. products resulting from ozonolysis of human breath and from reaction of O_3 with standard compounds (Table S6). The two most prominent products produced by the reactions of O_3 with isoprene and α-terpinene were A_{10} or B_{10} (104–125 pptv) which formation is described below in the "reaction mechanism".

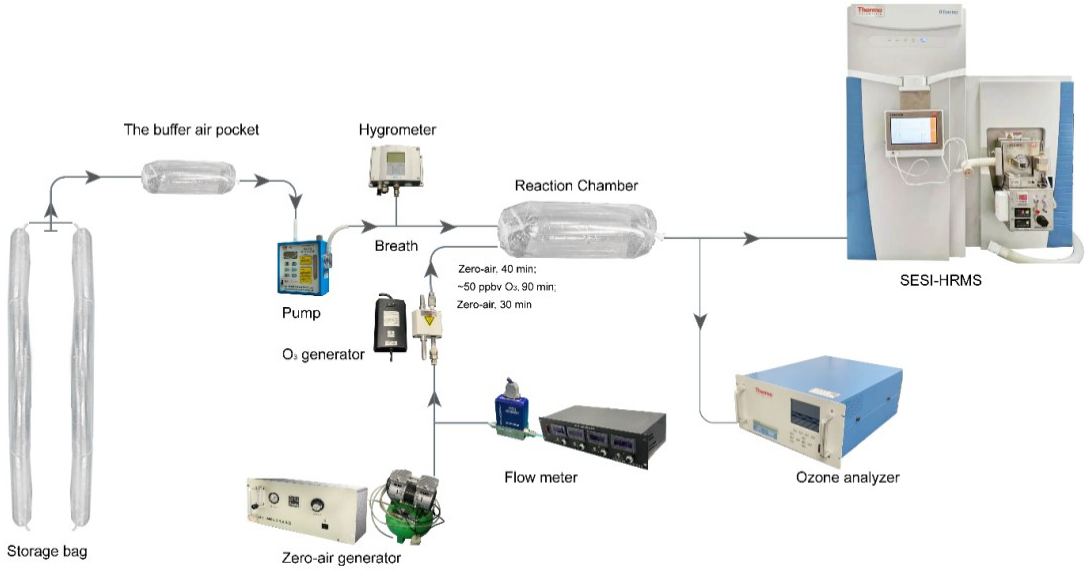

Figure S1. Experimental set-up for real-time monitoring of ozone (O_3) reaction with exhaled human breath.

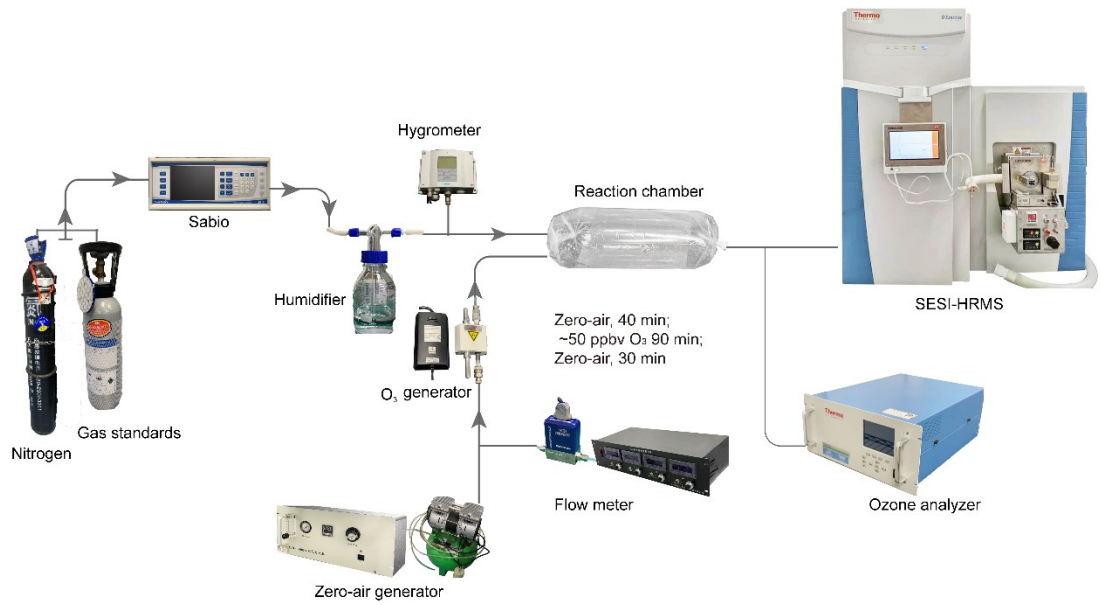

Figure S2. Experimental set-up for real-time monitoring of O_3 reaction with standard compounds which are typical VOCs identified in human breath.

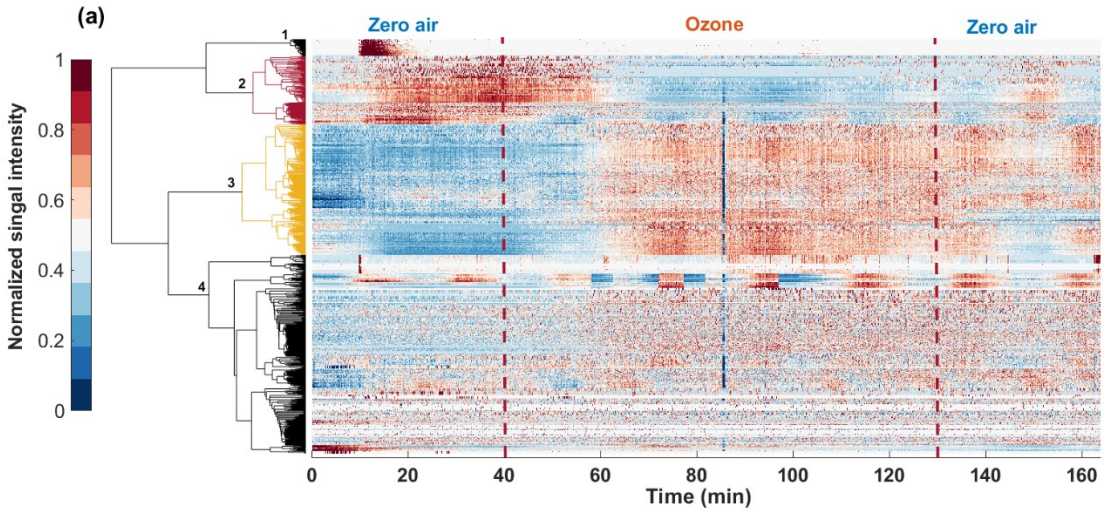

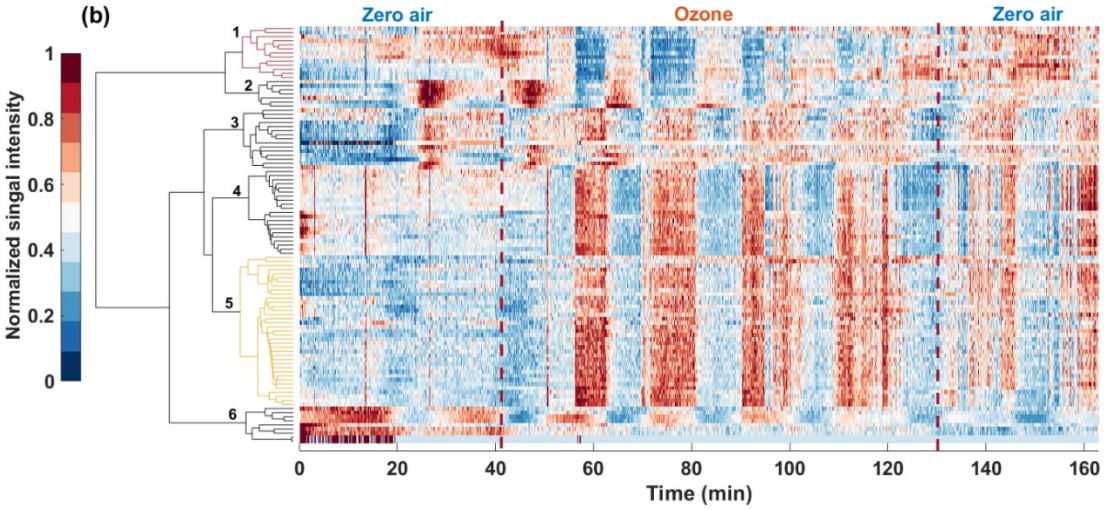

Figure S3. Hierarchical cluster analysis of (a) 694 ions detected in the positive ion detection mode and (b) 102 ions detected in the negative ion detection mode. The normalized signal intensity in hierarchical cluster is presented by a color-coded scale, i.e., the signal intensity increases from dark blue (normalized value is 0) to wine red (normalized value is 1). It should be noted that the periodic fluctuations of signal intensities over time in Figure S3a Cluster 4 and Figure S3b are due to the MS/MS analyses performed for these ions at certain time periods.

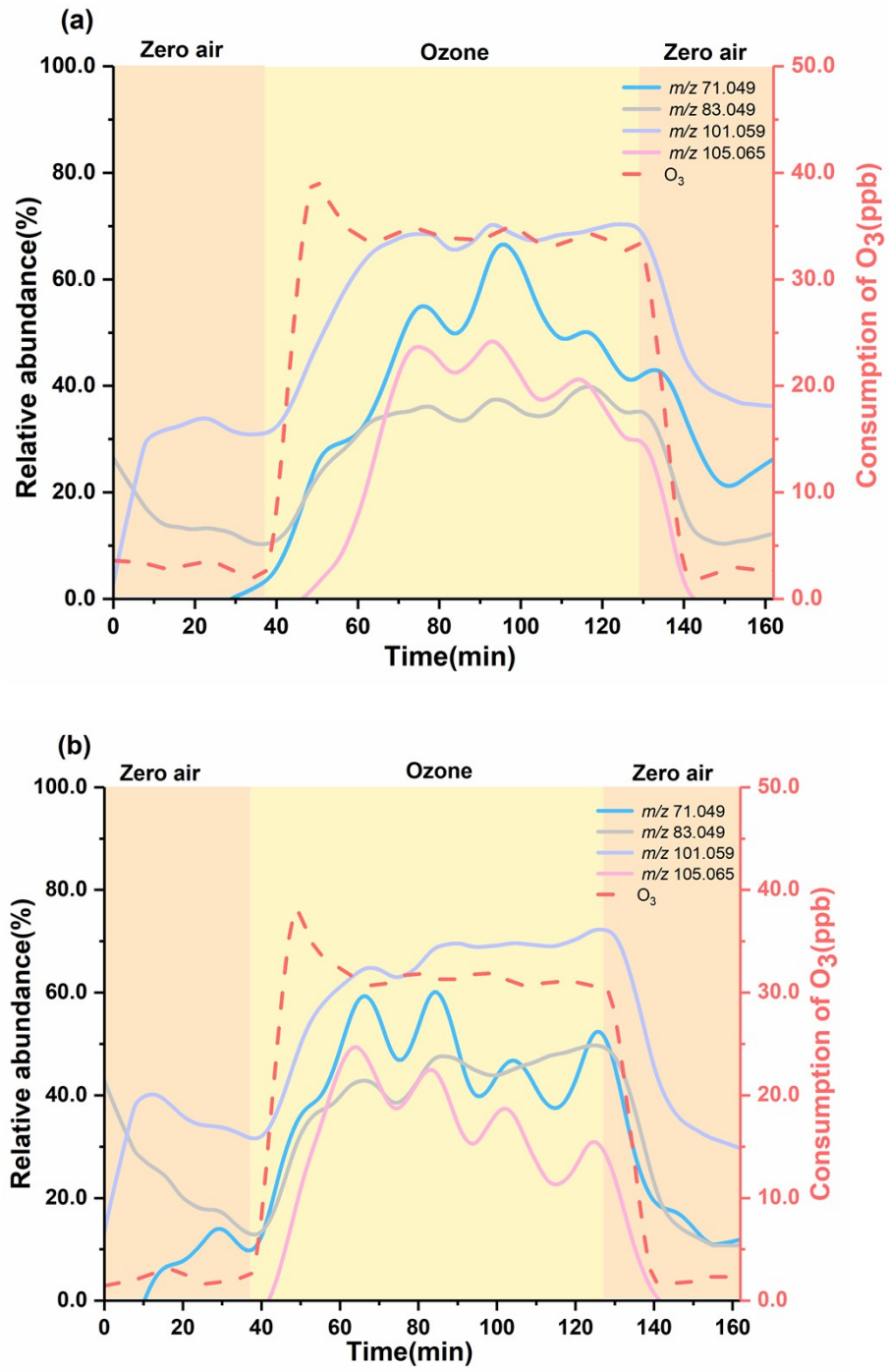
(a)
Zero air
Ozone
Zero air
m/z 71.049
m/z 83.049
m/z 101.059
m/z 105.065
O3
Relative abundance(%)
Consumption of O3(ppb)
Time(min)
(b)
Zero air
Ozone
Zero air
m/z 71.049
m/z 83.049
m/z 101.059
m/z 105.065
O3
Relative abundance(%)
Consumption of O3(ppb)
Time(min)

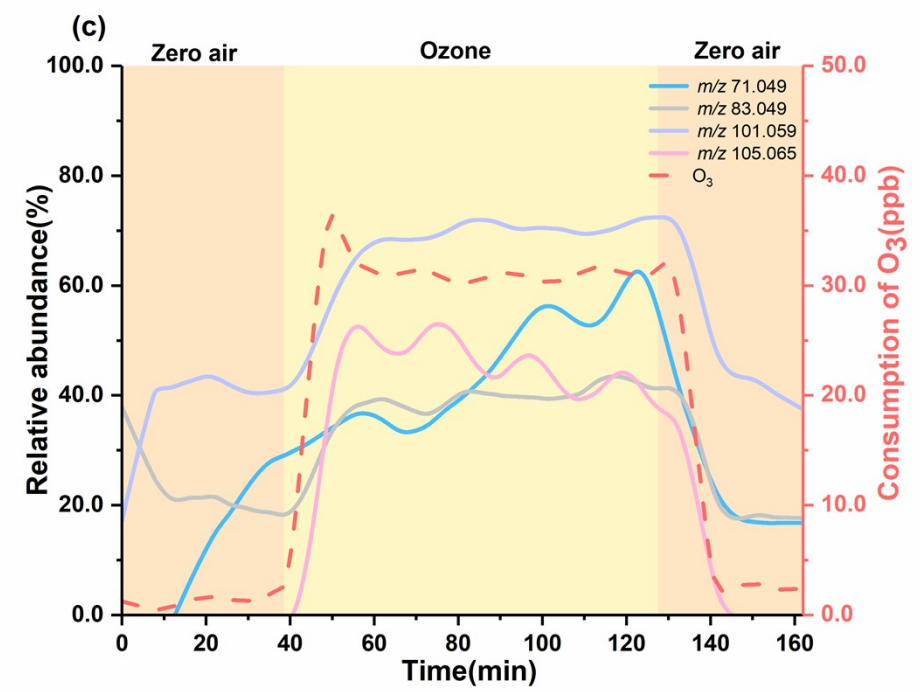

Figure S4. Intensity-time profiles (solid lines) of ions detected in positive mode and time profile (dash line) of O_3 mixing ratio for human breath samples (a) YZH-Pos, (b) CX-Pos and (c) LC-Pos, relative abundance is defined as the intensity of each ion normalized to the highest intensity during the full course of reaction.

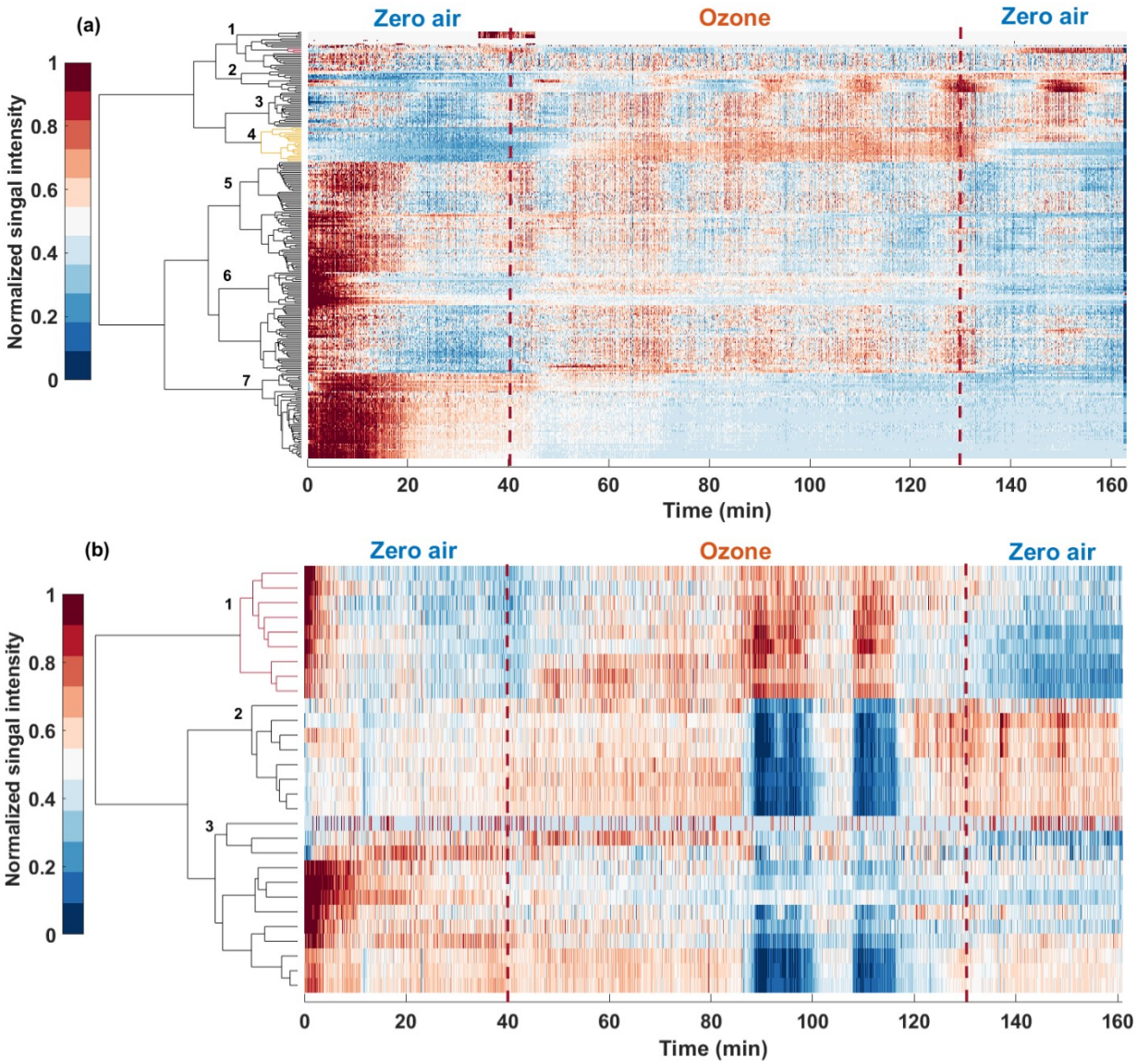

Figure S5. Hierarchical cluster analysis of ions produced by the reaction of O_3 and standard isoprene in (a) positive mode and (b) negative mode. The normalized signal intensity in hierarchical cluster is presented by a color-coded scale, i.e., the signal intensity increases from dark blue (normalized value is 0) to wine red (normalized value is 1).

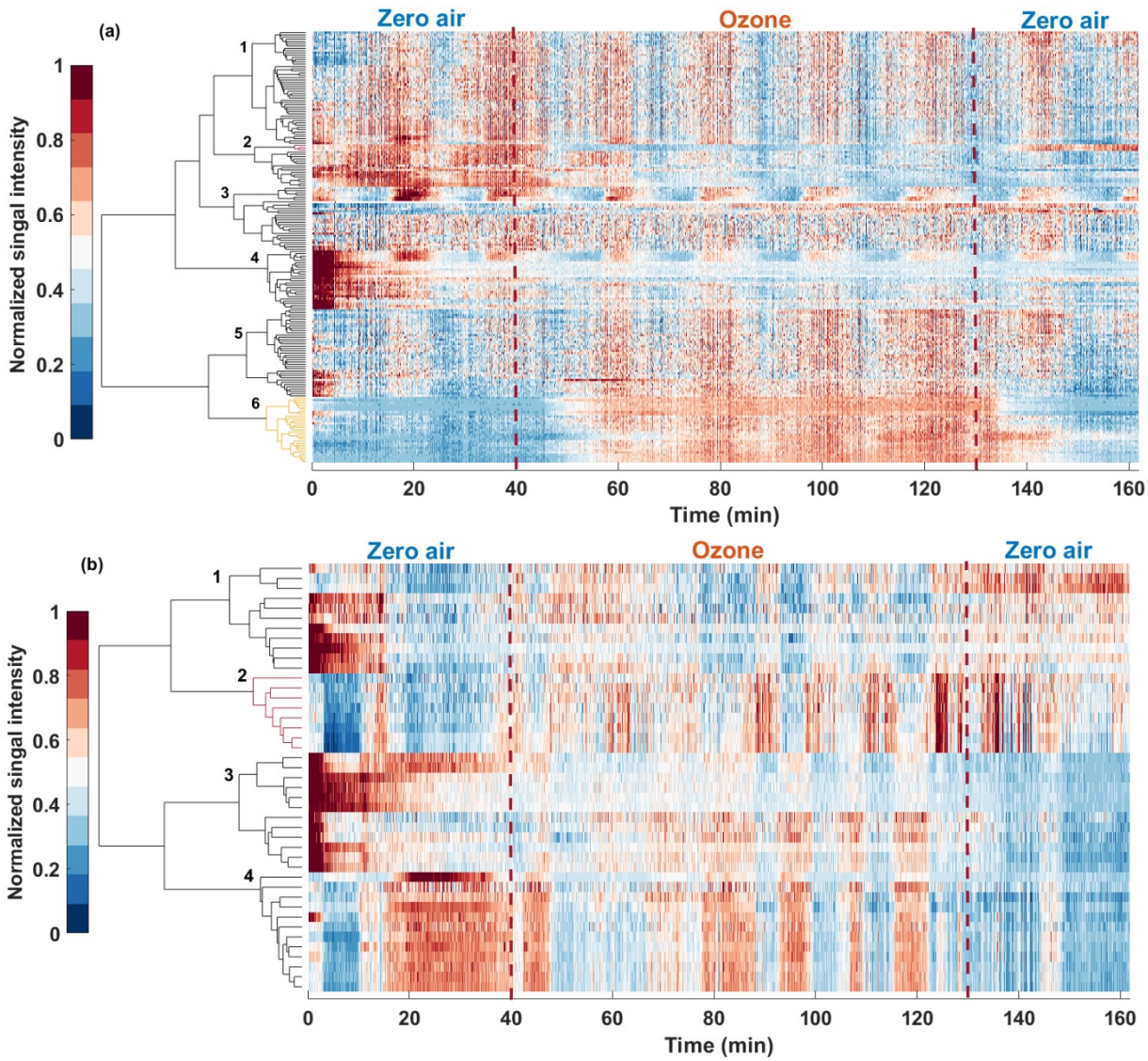

Figure S6. Hierarchical cluster analysis of ions produced by the reaction of O_3 and standard α-terpinene in (a) positive mode and (b) negative mode. The normalized signal intensity in hierarchical cluster is presented by a color-coded scale, i.e., the signal intensity increases from dark blue (normalized value is 0) to wine red (normalized value is 1).

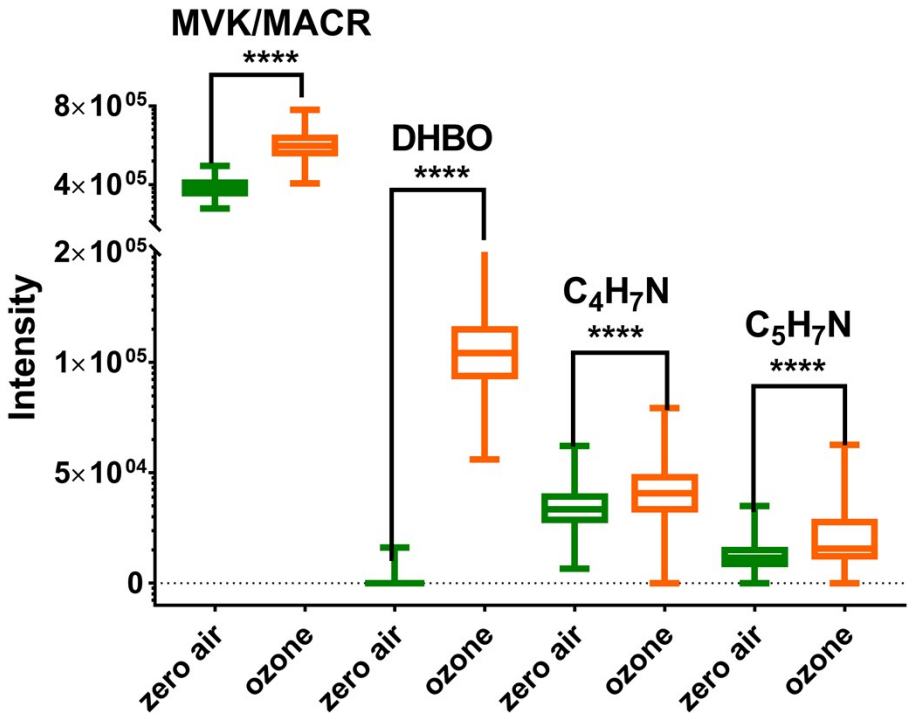

Figure S7. The box plot of MVK, MACR, DHBO and the imine compounds.

Table S1. Mixing ratios and RH values of simulated breath samples prepared using two individual standard gases.

Parameters	Samples	Value
RH	All simulated samples	92%–94%
Mixing ratio	Isoprene	730 pptv
	α-terpinene	410 pptv

Table S2. The mixing ratios of isoprene and α-terpinene in 9 subjects breath samples.

Subject	Subject Mixing ratio (ppbv)	
	Isoprene	α-Terpinene
1	0.74	0.17
2	1.16	0.17
3	1.83	0.67
4	0.67	0.73
5	0.38	0.24
6	0.40	0.66
7	0.80	0.39
8	0.42	0.29
9	0.20	0.17
AVE	0.73	0.39

[a]Results of subjects 5–9 are from other experiments.

Table S3. Number of ions detected by SESI-HRMS for four subjects.

Subject	Detection mode	No. of ions	No. of product ions[c]
YZH	Pos[a]	694	219
	Neg[b]	124	3
CX	Pos	831	44
	Neg	112	16
LC	Pos	851	42
	Neg	131	24
XX	Pos	618	62
	Neg	102	37

[a]Pos: position ion detection mode; [b]Neg: negative ion detection mode; [c]product ions: ions that showed an increasing trend at O_3 exposure stage.

Table S4. CHON compounds identified resulting from the reaction of O_3 and exhaled breath in positive (cluster 3 in figure S3a) and negative mode (cluster 5 in figure S3b).

No.	Mode	DBE	*m/z*	Formula	No.	Mode	DBE	*m/z*	Formula
1	Positive	2	58.974	CHO_2N	**2**	Positive	1	59.036	C_2H_5ON
3	Positive	0.5	60.044	C_2H_6ON	**4**	Positive	0	61.053	C_2H_7ON
5	Positive	0	61.055	C_2H_7ON	**6**	Positive	0.5	88.075	$C_4H_{10}ON$
7	Positive	0.5	104.07	$C_4H_{10}O_2N$	**8**	Positive	0.5	105.065	$C_3H_9O_2N_2$
9	Positive	1.5	114.091	$C_6H_{12}ON$	**10**	Positive	1.5	114.092	$C_6H_{12}ON$
11	Positive	1.5	115.088	$C_5H_{11}ON_2$	**12**	Positive	4.5	115.094	$C_4H_{11}N_4$
13	Positive	0.5	116.095	$C_5H_{12}ON_2$	**14**	Positive	2	116.098	$C_5H_{12}ON_2$
15	Positive	0.5	116.106	$C_6H_{14}ON$	**16**	Positive	1	118.086	$C_5H_{12}O_2N$
17	Positive	0.5	119.083	$C_4H_{11}O_2N_2$	**18**	Positive	0	120.088	$C_4H_{12}O_2N_2$
19	Positive	0	122.068	$C_3H_{10}O_3N_2$	**20**	Positive	1.5	128.106	$C_7H_{14}ON$
21	Positive	10	133.067	CH_7ON_7	**22**	Positive	1	148.083	$C_5H_{12}O_3N_2$
23	Positive	12	207.029	$C_{13}H_5O_2N$	**24**	Positive	12	207.03	$C_{13}H_5O_2N$
25	Positive	12	207.031	$C_{13}H_5O_2N$	**26**	Positive	0	222.156	$C_9H_{22}O_4N_2$
27	Positive	11	223.063	$C_{14}H_9O_2N$	**28**	Positive	2.5	224.063	$C_4H_{10}O_6N_5$
29	Positive	6.5	224.066	$C_9H_{10}O_4N_3$	**30**	Positive	11	225.042	$C_{13}H_7O_3N$
31	Positive	7	225.06	$C_6H_7O_3N_7$	**32**	Positive	2.5	227.175	$C_{12}H_{23}O_2N_2$
33	Positive	11	229.001	$C_{11}H_3O_5N$	**34**	Positive	3.5	252.195	$C_{15}H_{26}O_2N$
35	Positive	9.5	268.978	$C_7HO_8N_4$	**36**	Positive	5.5	277.216	$C_{18}H_{29}O_2$
37	Positive	12.5	282.049	$C_{14}H_8O_4N_3$	**38**	Positive	12.5	282.05	$C_{14}H_8O_4N_3$
39	Positive	8.5	283.029	$C_9H_7O_7N_4$	**40**	Positive	8.5	283.03	$C_9H_7O_7N_4$
41	Positive	7.5	297.082	$C_{11}H_{13}O_6N_4$	**42**	Positive	11.5	298.082	$C_{15}H_{12}O_4N_3$
43	Positive	15.5	298.085	$C_{20}H_{12}O_2N$	**44**	Positive	7.5	299.061	$C_{10}H_{11}O_7N_4$
45	Positive	11	299.078	$C_{16}H_{13}O_5N$	**46**	Positive	11	299.079	$C_{16}H_{13}O_5N$
47	Positive	15.5	300.064	$C_{19}H_{10}O_3N$	**48**	Positive	15.5	300.065	$C_{19}H_{10}O_3N$
49	Positive	11	301.057	$C_{15}H_{11}O_6N$	**50**	Positive	11	301.058	$C_{15}H_{11}O_6N$
51	Positive	19	341.017	$C_{17}H_3O_4N_5$	**52**	Positive	19	341.018	$C_{17}H_3O_4N_5$
53	Positive	19	342.997	$C_{16}HO_5N_5$	**54**	Positive	19	342.998	$C_{16}HO_5N_5$
55	Positive	6.5	344.976	$CHO_{12}N_{10}$	**56**	Positive	18	357.049	$C_{18}H_7O_4N_5$
57	Positive	18	359.027	$C_{17}H_5O_5N_5$	**58**	Positive	18	359.028	$C_{17}H_5O_5N_5$
59	Positive	22	360.027	$C_{21}H_4O_3N_4$	**60**	Positive	22	360.028	$C_{21}H_4O_3N_4$
61	Positive	16	388.126	$C_{20}H_{16}O_3N_6$	**62**	Positive	16	388.127	$C_{20}H_{16}O_3N_6$

63	Positive	16	388.128	$C_{20}H_{16}O_3N_6$	**64**	Positive	16	389.111	$C_{20}H_{15}O_4N_5$
65	Positive	16	389.112	$C_{20}H_{15}O_4N_5$	**66**	Positive	10.5	415.035	$C_{13}H_{11}O_{12}N_4$
67	Positive	10.5	415.036	$C_{13}H_{11}O_{12}N_4$	**68**	Positive	10.5	415.037	$C_{13}H_{11}O_{12}N_4$
69	Positive	9.5	429.088	$C_{15}H_{17}O_{11}N_4$	**70**	Positive	19	430.086	$C_{18}H_{10}O_4N_{10}$
71	Positive	19	430.087	$C_{18}H_{10}O_4N_{10}$	**72**	Positive	19	430.088	$C_{18}H_{10}O_4N_{10}$
73	Positive	19	430.089	$C_{18}H_{10}O_4N_{10}$	**74**	Positive	9.5	431.067	$C_{14}H_{15}O_{12}N_4$
75	Positive	9.5	431.068	$C_{14}H_{15}O_{12}N_4$	**76**	Positive	9.5	431.069	$C_{14}H_{15}O_{12}N_4$
77	Positive	18	431.084	$C_{21}H_{13}O_6N_5$	**78**	Positive	18	431.085	$C_{21}H_{13}O_6N_5$
79	Positive	18	431.086	$C_{21}H_{13}O_6N_5$	**80**	Positive	18	431.088	$C_{21}H_{13}O_6N_5$
81	Positive	13.5	432.067	$C_{18}H_{14}O_{10}N_3$	**82**	Positive	13.5	432.068	$C_{18}H_{14}O_{10}N_3$
83	Positive	13.5	432.069	$C_{18}H_{14}O_{10}N_3$	**84**	Positive	18	433.064	$C_{20}H_{11}O_7N_5$
85	Positive	18	433.065	$C_{20}H_{11}O_7N_5$	**86**	Positive	18	433.066	$C_{20}H_{11}O_7N_5$
87	Positive	3.5	448.115	$C_{11}H_{22}O_{14}N_5$	**88**	Positive	3.5	448.116	$C_{11}H_{22}O_{14}N_5$
89	Positive	3.5	448.117	$C_{11}H_{22}O_{14}N_5$	**90**	Positive	1.5	448.349	$C_{21}H_{46}O_5N_5$
91	Positive	1.5	448.35	$C_{21}H_{46}O_5N_5$	**92**	Positive	1.5	448.351	$C_{21}H_{46}O_5N_5$
93	Positive	1.5	448.352	$C_{21}H_{46}O_5N_5$	**94**	Positive	8	449.112	$C_{13}H_{19}O_{11}N_7$
95	Positive	8	449.113	$C_{13}H_{19}O_{11}N_7$	**96**	Positive	8	449.114	$C_{13}H_{19}O_{11}N_7$
97	Positive	8	449.118	$C_{13}H_{19}O_{11}N_7$	**98**	Positive	8	449.119	$C_{13}H_{19}O_{11}N_7$
99	Positive	8	449.121	$C_{13}H_{19}O_{11}N_7$	**100**	Positive	8	449.122	$C_{13}H_{19}O_{11}N_7$
101	Positive	12	450.112	$C_{17}H_{18}O_9N_6$	**102**	Positive	12	450.113	$C_{17}H_{18}O_9N_6$
103	Positive	12	450.114	$C_{17}H_{18}O_9N_6$	**104**	Positive	12	450.115	$C_{17}H_{18}O_9N_6$
105	Positive	7.5	462.146	$C_{16}H_{24}O_{11}N_5$	**106**	Positive	11.5	463.144	$C_{20}H_{23}O_9N_4$
107	Positive	11.5	463.145	$C_{20}H_{23}O_9N_4$	**108**	Positive	11	463.146	$C_{20}H_{23}O_9N_4$
109	Positive	11	464.142	$C_{21}H_{24}O_{10}N_2$	**110**	Positive	10.5	464.15	$C_{21}H_{24}O_{10}N_2$
111	Positive	11	464.151	$C_{21}H_{24}O_{10}N_2$	**112**	Positive	2.5	465.14	$C_{11}H_{25}O_{14}N_6$
113	Positive	2.5	465.141	$C_{11}H_{25}O_{14}N_6$	**114**	Positive	2.5	465.143	$C_{11}H_{25}O_{14}N_6$
115	Positive	2.5	465.144	$C_{11}H_{25}O_{14}N_6$	**116**	Positive	2.5	465.146	$C_{11}H_{25}O_{14}N_6$
117	Positive	2.5	465.147	$C_{11}H_{25}O_{14}N_6$	**118**	Positive	2.5	465.149	$C_{11}H_{25}O_{14}N_6$
119	Positive	2.5	465.15	$C_{11}H_{25}O_{14}N_6$	**120**	Positive	19.5	466.138	$C_{27}H_{20}O_5N_3$
121	Positive	19.5	466.14	$C_{27}H_{20}O_5N_3$	**122**	Positive	19.5	466.141	$C_{27}H_{20}O_5N_3$
123	Positive	19.5	466.144	$C_{27}H_{20}O_5N_3$	**124**	Positive	15	466.146	$C_{23}H_{22}O_7N_4$
125	Positive	15	466.147	$C_{23}H_{22}O_7N_4$	**126**	Positive	15	466.148	$C_{23}H_{22}O_7N_4$
127	Positive	15	466.149	$C_{23}H_{22}O_7N_4$	**128**	Positive	11	486.258	$C_{24}H_{34}O_5N_6$
129	Positive	11	486.259	$C_{24}H_{34}O_5N_6$	**130**	Positive	20	489.054	$C_{22}H_{11}O_9N_5$
131	Positive	20	489.055	$C_{22}H_{11}O_9N_5$	**132**	Positive	20	489.056	$C_{22}H_{11}O_9N_5$
133	Negative	5.5	138.019	$C_6H_4O_3N$	**134**	Negative	6.5	149.045	$C_6H_5ON_4$
135	Negative	3	224.027	$C_5H_8O_8N_2$	**136**	Negative	7.5	225.025	$C_7H_5O_5N_4$
137	Negative	5.5	250.144	$C_{14}H_{20}O_3N$	**138**	Negative	13.5	297.047	$C_{11}H_5O_3N_8$
139	Negative	13.5	299.026	$C_{10}H_3O_4N_8$					

Table S5. CHO compounds identified resulting from the reaction of O_3 and breath in positive (cluster 3 in figure S3a) and negative mode (cluster 5 in figure S3b).

No.	Mode	DBE	*m/z*	Formula	No.	Mode	DBE	*m/z*	Formula
1	Positive	0.5	59.049	C_3H_7O	**2**	Positive	0.5	59.05	C_3H_7O
3	Positive	0.5	59.053	C_3H_7O	**4**	Positive	0.5	59.054	C_3H_7O
5	Positive	0.5	61.028	$C_2H_5O_2$	**6**	Positive	1.5	71.049	C_4H_7O
7	Positive	1.5	73.028	$C_3H_5O_2$	**8**	Positive	0.5	73.064	C_4H_9O
9	Positive	0.5	75.044	$C_3H_7O_2$	**10**	Positive	2.5	83.049	C_5H_7O
11	Positive	2.5	85.028	$C_4H_5O_2$	**12**	Positive	1.5	85.064	C_5H_9O
13	Positive	1.5	87.044	$C_4H_7O_2$	**14**	Positive	0.5	87.08	$C_5H_{11}O$
15	Positive	0.5	89.059	$C_4H_9O_2$	**16**	Positive	3.5	95.049	C_6H_7O
17	Positive	2.5	97.064	C_6H_9O	**18**	Positive	2.5	99.043	$C_5H_7O_2$
19	Positive	2.5	99.044	$C_5H_7O_2$	**20**	Positive	1.5	99.08	$C_6H_{11}O$
21	Positive	1.5	101.059	$C_5H_9O_2$	**22**	Positive	5.5	105.036	C_7H_5O
23	Positive	4.5	107.049	C_7H_7O	**24**	Positive	3.5	109.064	C_7H_9O
25	Positive	2.5	111.08	$C_7H_{11}O$	**26**	Positive	2.5	113.059	$C_6H_9O_2$
27	Positive	1.5	113.096	$C_7H_{13}O$	**28**	Positive	1.5	115.075	$C_6H_{11}O_2$
29	Positive	0.5	115.111	$C_7H_{15}O$	**30**	Positive	0.5	117.09	$C_6H_{13}O_2$
31	Positive	4.5	121.064	C_8H_9O	**32**	Positive	4.5	123.043	$C_7H_7O_2$
33	Positive	3.5	123.079	$C_8H_{11}O$	**34**	Positive	3.5	123.08	$C_8H_{11}O$
35	Positive	3.5	125.059	$C_7H_9O_2$	**36**	Positive	2.5	125.096	$C_8H_{13}O$
37	Positive	2.5	127.075	$C_7H_{11}O_2$	**38**	Positive	0.5	127.111	$C_8H_{15}O$
39	Positive	1.5	129.09	$C_7H_{13}O_2$	**40**	Positive	5.5	133.064	C_9H_9O
41	Positive	4.5	137.059	$C_8H_9O_2$	**42**	Positive	3.5	137.096	$C_9H_{13}O$
43	Positive	3.5	139.075	$C_8H_{11}O_2$	**44**	Positive	2.5	141.09	$C_8H_{13}O_2$
45	Positive	1.5	141.127	$C_9H_{17}O$	**46**	Positive	1.5	143.106	$C_8H_{15}O_2$
47	Positive	0.5	145.122	$C_8H_{17}O_2$	**48**	Positive	1.5	147.064	$C_6H_{11}O_4$
49	Positive	5.5	147.08	$C_{10}H_{11}O$	**50**	Positive	1.5	149.044	$C_5H_9O_5$
51	Positive	4.5	149.096	$C_{10}H_{13}O$	**52**	Positive	3.5	151.111	$C_{10}H_{15}O$
53	Positive	3.5	153.09	$C_9H_{13}O_2$	**54**	Positive	2.5	153.127	$C_{10}H_{17}O$
55	Positive	2.5	155.106	$C_9H_{15}O_2$	**56**	Positive	1.5	157.122	$C_9H_{17}O_2$
57	Positive	6.5	163.038	$C_9H_7O_3$	**58**	Positive	4.5	163.111	$C_{11}H_{15}O$
59	Positive	4.5	165.09	$C_{10}H_{13}O_2$	**60**	Positive	0.5	167.055	$C_5H_{11}O_6$
61	Positive	3.5	167.106	$C_{10}H_{15}O_2$	**62**	Positive	0.5	169.034	$C_4H_9O_7$
63	Positive	2.5	169.122	$C_{10}H_{17}O_2$	**64**	Positive	3.5	193.158	$C_{13}H_{21}O$
65	Positive	3.5	207.174	$C_{14}H_{23}O$	**66**	Positive	4.5	219.174	$C_{15}H_{23}O$

67	Positive	4.5	221.153	$C_{14}H_{21}O_2$	**68**	Positive	3.5	221.189	$C_{15}H_{25}O$
69	Positive	4.5	235.169	$C_{15}H_{23}O_2$	**70**	Positive	3.5	237.184	$C_{15}H_{25}O_2$
71	Positive	3.5	281.049	$C_9H_{13}O_{10}$	**72**	Positive	3.5	281.05	$C_9H_{13}O_{10}$
73	Positive	3.5	361.024	$C_9H_{13}O_{15}$	**74**	Positive	3.5	361.025	$C_9H_{13}O_{15}$
75	Positive	3.5	361.026	$C_9H_{13}O_{15}$	**76**	Positive	5.5	447.345	$C_{28}H_{47}O_4$
77	Positive	5.5	447.346	$C_{28}H_{47}O_4$	**78**	Positive	1	486.267	$C_{21}H_{42}O_{12}$
79	Negative	1.5	59.013	$C_2H_3O_2$	**80**	Negative	2.5	69.034	C_4H_5O
81	Negative	2.5	71.013	$C_3H_3O_2$	**82**	Negative	1.5	71.05	C_4H_7O
83	Negative	2.5	72.993	C_2HO_3	**84**	Negative	2.5	72.993	C_2HO_3
85	Negative	1.5	73.029	$C_3H_5O_2$	**86**	Negative	1.5	75.008	$C_2H_3O_3$
87	Negative	3.5	81.034	C_5H_5O	**88**	Negative	2.5	83.05	C_5H_7O
89	Negative	2.5	85.029	$C_4H_5O_2$	**90**	Negative	2.5	87.008	$C_3H_3O_3$
91	Negative	1.5	87.045	$C_4H_7O_2$	**92**	Negative	2.5	99.045	$C_5H_7O_2$
93	Negative	2.5	101.024	$C_4H_5O_3$	**94**	Negative	1.5	103.04	$C_4H_7O_3$
95	Negative	4.5	109.029	$C_6H_5O_2$	**96**	Negative	3.5	113.024	$C_5H_5O_3$
97	Negative	2.5	115.04	$C_5H_7O_3$	**98**	Negative	1.5	117.055	$C_5H_9O_3$
99	Negative	4.5	125.024	$C_6H_5O_3$	**100**	Negative	3.5	127.04	$C_6H_7O_3$
101	Negative	2.5	129.055	$C_6H_9O_3$	**102**	Negative	2.5	143.071	$C_7H_{11}O_3$
103	Negative	4.5	151.076	$C_9H_{11}O_2$	**104**	Negative	3.5	155.071	$C_8H_{11}O_3$
105	Negative	2.5	157.086	$C_8H_{13}O_3$	**106**	Negative	2.5	157.087	$C_8H_{13}O_3$
107	Negative	1.5	159.102	$C_8H_{15}O_3$	**108**	Negative	4.5	167.071	$C_9H_{11}O_3$
109	Negative	3.5	169.087	$C_9H_{13}O_3$	**110**	Negative	2.5	171.102	$C_9H_{15}O_3$
111	Negative	5.5	179.071	$C_{10}H_{11}O_3$	**112**	Negative	2.5	185.082	$C_8H_{13}O_3$
113	Negative	8.5	201.055	$C_{12}H_9O_3$	**114**	Negative	5	236.141	$C_{14}H_{20}O_3$

Table S6. Compounds identified resulting from the reaction of O_3 and individual gas standards.

No.	STD	Compound	formula	Ion mode	Elemental composition	*m/z*	Δmmu	Mixing ratio (pptv)[a]
1	Isoprene	A10	$C_5H_8O_2$	$[M+H]^+$	$C_5H_9O_2$	101.059	−0.036	121
2		Product 1	$C_3H_2O_3$	$[M-H]^-$	C_3HO_3	84.990	−2.427	1479
3		3-Methylfuran	C_5H_6O	$[M+H]^+$	C_5H_7O	83.049	−0.061	26
4		A10	$C_5H_8O_2$	$[M+H]^+(^{13}C)$	$C_4{}^{13}CH_9O_2$	102.063	−0.041	6
5		Product 2	$C_9H_{14}O_2$	$[M+H]^+$	$C_9H_{15}O_2$	155.106	−0.056	8
				$[M+H-H_2O]^+$	$C_9H_{13}O$	137.096	0.028	12
6		Product 3	$C_{10}H_{14}O_2$	$[M+H]^+$	$C_{10}H_{15}O_2$	167.106	0.024	11
7		Product 4	$C_{15}H_{23}O$	$[M+H]^+$	$C_{15}H_{24}O$	220.182	−0.097	40
				$[M+H]^+(^{13}C)$	$C_{14}{}^{13}CH_{24}O$	221.185	−0.072	6
8		Product 5	$C_2H_4O_3$	$[M-H]^-$	$C_2H_3O_3$	75.008	0.013	77
9		Product 6	$C_4H_2O_4$	$[M-H]^-$	C_4HO_4	112.985	−2.412	41

10		Product 7	$C_5H_8O_3$	$[M-H]^-$	$C_5H_7O_3$	115.040	−0.007	9
11		Product 8	$C_6H_{10}O_3$	$[M-H]^-$	$C_6H_9O_3$	129.055	0.053	34
12		Product 9	$C_2H_2O_6N_3$	$[M-H]^-$	$C_2HO_6N_3$	162.982	−4.643	41
13	α-Terpinene	B10	$C_5H_8O_2$	$[M+H]^+$	$C_5H_9O_2$	101.059	−0.026	124
14		Product 10	CH_2O_3	$[M-H]^-$	CHO_3	60.993	0.023	543
15		Product 11	CH_3O_4	$[M-H]^-$	CH_2O_4	77.991	−4.476	1206
16		Product 12	CH_2O_4	$[M-H]^-$	CHO_4	76.988	0.038	2178
17		Product 13	CH_3O_3	$[M-H]^-$	CH_2O_3	61.996	−4.722	709
				$[M+H-H_2O]^+$	C_5H_7O	83.049	−0.061	27
18		Product 14	$C_7H_8O_2$	$[M+H]^+$	$C_7H_9O_2$	125.059	0.054	7
19		Product 15	$C_{10}H_{16}O_3$	$[M+H-H_2O]^+$	$C_{10}H_{15}O_2$	167.106	0.034	22
20		Product 16	$C_{15}H_{23}O$	$[M+H]^+$	$C_{15}H_{24}O$	220.182	−0.087	38
				$[M+H]^+(^{13}C)$	$C_{14}{}^{13}CH_{24}O$	221.185	−0.072	6

21	Product 17	CHO_3	$[M-H]^-$	CO_3	59.985	0.008	19
			$[M-H]^-(^{13}C)$	$^{13}CO_3$	60.988	0.133	14
22	Product 18	H_2O_4N	$[M-H]^-$	HO_4N	78.992	1.174	36
23	Product 19	$C_{16}H_{32}O_2$	$[M-H]^-$	$C_{16}H_{31}O_2$	255.232	−0.124	13

[a]The mixing ratio of each product compound was calculated as follows: $C_{i,\ \mathrm{breath}}-C_{i,\ \mathrm{blank}}$, where $C_{i,\ \mathrm{breath}}$ is the mixing ratio of compound i in breath and $C_{i,\ \mathrm{blank}}$ is the mixing ratio of compound i in the blank sample

References

1. J. Zeng, M. Mekic, X. Xu, G. Loisel, Z. Zhou, S. Gligorovski and X. Li, A novel insight into the ozone-skin lipid oxidation products observed by secondary electrospray ionization high-resolution mass spectrometry, *Environ. Sci. Technol.*, 2020, **54**, 13478–13487.
2. T. K. Kim, T test as a parametric statistic, *Korean J. Anesthesiol.*, 2015, **68**, 540–546.
3. M. M. Yassine, M. Harir, E. Dabek-Zlotorzynska and P. Schmitt-Kopplin, Structural characterization of organic aerosol using Fourier transform ion cyclotron resonance mass spectrometry: Aromaticity equivalent approach, *Rapid Commun. Mass Spectrom.*, 2014, **28**, 2445–2454.
4. I. Kourtchev, R. H. M. Godoi, S. Connors, J. G. Levine, A. T. Archibald, A. F. L. Godoi, S. L. Paralovo, C. G. G. Barbosa, R. A. F. Souza, A. O. Manzi, R. Seco, S. Sjostedt, J. H. Park, A. Guenther, S. Kim, J. Smith, S. T. Martin and M. Kalberer, Molecular composition of organic aerosols in central amazonia: an ultra-high-resolution mass spectrometry study, *Atmos. Chem. Phys.*, 2016, **16**, 11899–11913.
5. X. Wang, N. Hayeck, M. Brüggemann, L. Yao, H. Chen, C. Zhang, C. Emmelin, J. Chen, C. George and L. Wang, Chemical characteristics of organic aerosols in Shanghai: a Study by ultrahigh-performance liquid chromatography coupled with orbitrap mass spectrometry, *J. Geophys. Res. Atmos.*, 2017, **122**, 11,703-11,722.
6. M. Mekic, J. Zeng, B. Jiang, X. Li, Y. G. Lazarou, M. Brigante, H. Herrmann and S. Gligorovski, Formation of toxic unsaturated multifunctional and organosulfur compounds from the photosensitized processing of fluorene and DMSO at the air-water interface, *J. Geophys. Res. Atmos.*, 2020, **125**, e2019JD031839.

7. Y. Wang, M. Mekic, P. Li, H. Deng, S. Liu, B. Jiang, B. Jin, D. Vione and S. Gligorovski, Ionic strength effect triggers brown carbon formation through heterogeneous ozone processing of ortho-vanillin, *Environ. Sci. Technol.*, 2021, **55**, 4553–4564.

8. H. J. Lee, P. K. Aiona, A. Laskin, J. Laskin and S. A. Nizkorodov, Effect of solar radiation on the optical properties and molecular composition of laboratory proxies of atmospheric brown carbon, *Environ. Sci. Technol.*, 2014, **48**, 10217–10226.

9. D. E. Romonosky, Y. Li, M. Shiraiwa, A. Laskin, J. Laskin and S. A. Nizkorodov, Aqueous photochemistry of secondary organic aerosol of α-pinene and α-humulene oxidized with ozone, hydroxyl radical, and nitrate radical, *J. Phys. Chem. A*, 2017, **121**, 1298–1309.

10. J. Song, M. Li, B. Jiang, S. Wei, X. Fan and P. Peng, Molecular characterization of water-soluble humic like substances in smoke particles emitted from combustion of eiomass materials and coal using ultrahigh-resolution electrospray ionization fourier transform ion cyclotron resonance mass spectrometry, *Environ. Sci. Technol.*, 2018, **52**, 2575–2585.

11. R. H. Perry, R. G. Cooks and R. J. Noll, Orbitrap mass spectrometry: instrumentation, ion motion and applications, *Mass Spectrom. Rev.*, 2008, **27**, 661–699.

12. B. R. G. Mabato, Y. Lyu, Y. Ji, D. D. Huang, X. Li, T. Nah, C. H. Lam and C. K. Chan, Aqueous SOA formation from the photo-oxidation of vanillin: direct photosensitized reactions and nitrate-mediated reactions, *Atmos. Chem. Phys. Discuss.*, 2021, **2021**, 1–35.